Sains Malaysiana 42(12)(2013): 1755–1761

Effect of Dissolution Times on Compressive Properties and Energy Absorption of Aluminum Foam

(Kesan Masa Pelarutan ke Atas Sifat Mampatan dan Penyerapan Tenaga Busa Aluminium)

NUR SURIANNI AHAMAD SUFFIN, ANASYIDA ABU SEMAN* & ZUHAILAWATI HUSSAIN

ABSTRACT

Aluminum foams were fabricated by sintering dissolution process (SDP) using sodium chloride (NaC_l) as space holder. The compositions of space holder, used in this study were 40 and 60 wt. % with different dissolution times; 1, 2 and 3 h. The effect of different dissolution times on compressive behavior and energy absorption of foams were evaluated. The result showed that by increasing space holder and dissolution times, energy absorption capability increases. For aluminum foam contains 60 wt. % NaC_l, longer dissolution times resulted in thinner cell wall and cell structure become more unstable which lead to lower plateau region.

Keywords: Aluminium foam; compressive properties; dissolution time; energy absorption; sintering dissolution process

ABSTRAK

Busa aluminium telah dihasilkan melalui proses pensinteran pelarutan (SDP) menggunakan natrium klorida (NaC_l) sebagai agen pembusaan. Komposisi bahan pembusaan yang digunakan dalam kajian ialah 40 dan 60 %berat dengan masa pembusaan yang berbeza; 1, 2 dan 3 jam. Kesan masa pembusaan yang berbeza ke atas sifat mampatan dan penyerapan tenaga aluminium berbusa dikaji. Hasil kajian menunjukkan dengan peningkatan agen pembusaan dan masa pelarutan, keupayaan penyerapan tenaga meningkat. Busa aluminium yang mengandungi 60 %berat NaC_l, dengan masa pelarutan yang lebih panjang menyebabkan dinding sel menjadi lebih nipis dan struktur sel menjadi lebih tidak stabil dan mengurangkan rantau dataran.

Kata kunci: Aluminium berbusa; masa pelarutan; penyerapan tenaga; proses pelarutan; proses pensinteran pelarutan

INTRODUCTION

The development in the production technology of metal foam materials is in such a great progress because metal foam has obtained obvious achievement in the metal industries (Haijun et al. 2007). This cellular structure which contained 75-95% volume of pores; made it possible to produce lightweight, strength and stiff-structure. With this combination of unique properties, metal foams has increased their potential for application in lightweight structural components, energy absorption systems and as heat exchanges in electronic devices (Andrews et al. 1999). Many researches (Cao et al. 2006; Miranda et al. 2010; Wang et al. 2006) have been carried out on metallic foams due to high demand in using metallic foam especially for automotive, railway, aerospace and chemical application. There were a number of studies on the properties of aluminum foam (Miranda et al. 2010; Zhang et al. 2010). According to Fusheng et al. (2004), composition and cell morphologies have influenced the mechanical properties of foams. Xiao-Qing et al. (2006) concluded that the compressive strength of foams not only depend on relative density but also depend on cell size and the foams cell size with larger modulus and higher strength under stress-strain curve. Bin et al. (2007) have studied the effect of pore size and relative density on the mechanical properties of open cell aluminum foams. Their research have highlighted that foam with lower density exhibited a longer flatter plateau which has higher energy absorption. The compressive stress-strain curve also increased with increasing pore size and relative density.

Many researchers (Cao et al. 2006; Xiao-Qing et al. 2006) have been developed on the improvement of the production processes to produce good quality foams with good properties. The current manufacturing methods were melting and powder metallurgy method. In this study, sintering dissolution process was used to fabricate the aluminum foams. Aluminum foams which were synthesized by the space holder method influenced by size and shape of the space holder. Gailard et al. (2004) found that the powder shape influence significantly the strain at which the foam stress-strain curve deviates from power-law behavior. It is demonstrated that the morphology and size of pores can be controlled by selecting an appropriate space holder particle. However, at certain amount of space holder that used in fabricated foam was not dissolved completely during the dissolution process. Zhao and Sun (2001) have reported that the space holder in contact with each other can be dissolved away by water, but there was small amount of residual space

holder particle in the resultant foam. In this study, NaC_l powder was used as space holder. Although NaC_l particle has a relatively high melting point and dissolve in water easily, NaC_l crystals were brittle (Mondal et al. 2009). As a result, NaC_l particles which were trapped in the resultant foam influenced the properties of the foam. Thus, it is important to ensure that the entire space holder particles were completely dissolved during the dissolution process. Due to this phenomenon, this paper investigated the effect of dissolution times on the morphology and mechanical properties of the aluminum foam.

Experimental Details

Pure aluminum powder with purity 99.8% and average size particles of 35 μm were used. NaC_l particles with average sizes of 1 mm were chosen as the space holder. The aluminum foams were fabricated by sintering dissolution process. The process mainly includes the mixing, compacting, sintering and removing foaming agent. The aluminum powders were mixed thoroughly with NaC_l particle in ball milling for an hour according to composition ratio; $60A_l$-$40NaC_l$ and $40A_l$-$60NaC_l$. A small amount of ethanol was added during milling to prevent the dissimilar powder from segregation. The mixture was pressed at 200 MPa into cylindrical compacts. The green compacts were sintered in tube furnace in argon atmosphere. The sintering temperature of the compacts was 570°C with 5 h soaking time. The NaC_l particles in the sample were removed by dissolved in hot water at 90°C with different dissolution times: 1, 2 and 3 h.

The density and porosity of the foams were calculated using (1) and (2):

$$\text{Foam density, } \rho_{foam} = \frac{w_a}{w_c - w_b} x\, \rho_{liquid}, \quad \rho_{liquid} = 1\, g/cm^3. \tag{1}$$

$$\text{Foam porosity, } \rho_{foam} = \left|1 - \left(\frac{\rho_f}{\rho_{Al}}\right)\right| x\, 100\%$$

$$\rho_{Al} = 2.7\ g/cm^3,\ \rho_f = \textit{foam density}. \tag{2}$$

The structure of aluminum foams, including cell morphology and microstructure were examined by Stereo Zoom optical microscope and Supra 35VP field emission scanning electron microscope (FESEM).

The compressive properties of the specimens were conducted on axial mechanical testing system at a crosshead speed of 1 mm/min at room temperature. The specimens for the compression test were 13 mm in diameter and 26 mm in height. The energy absorption of aluminum foams can be obtained from the area under the stress-strain curve using (3):

$$W = \int_0^{\varepsilon} \sigma\, d\varepsilon, \tag{3}$$

where W is the energy absorption capability and σ and ε are the compression stress and strain, respectively.

Results and Discussion

Figure 1 shows the effect of dissolution times on density and porosity of A_l-$40NaC_l$ and A_l-$60NaC_l$ foams. It is found that density of the foam decreased by increasing the duration of dissolution process. As been discussed by Zhao and Sun (2001), NaC_l particles were in contact with each other when high volume fraction of NaC_l was used. Since all NaC_l particles formed a continuous network in aluminum solid body, NaC_l particles can be dissolved away by water easily. However, the dissolution time must be long enough in order to dissolve all the NaC_l particles especially for foam prepared using high volume fraction of NaC_l. When foams with higher content of NaC_l were dipped in hot water for 1 h, there might be residual NaC_l

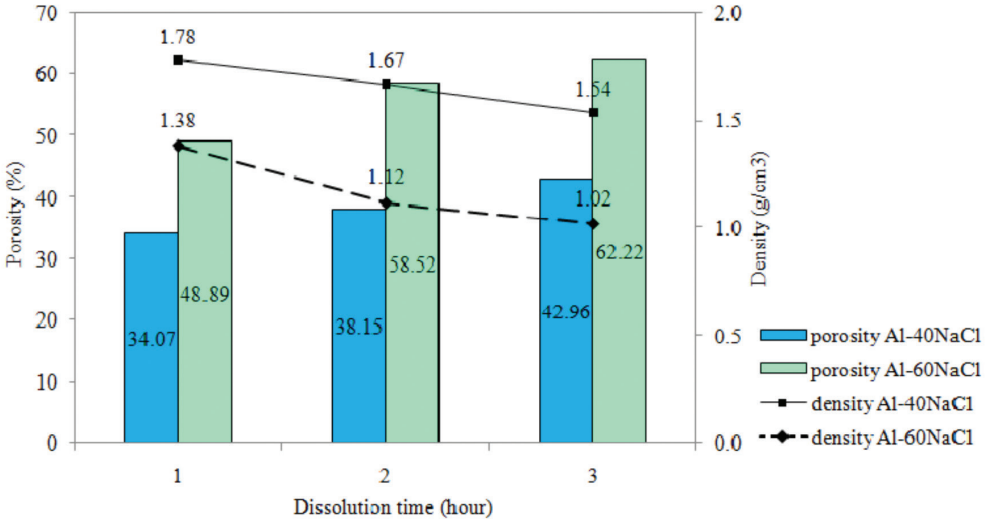

FIGURE 1. Density and porosity of aluminum foam with different dissolution times

particles in resultant foam since the dissolution time was too short. Consequently, the foam has low porosity because the NaC_l particles did not fully dissolve away in hot water and remained in the foam. These remaining NaC_l particles filled the parts that were supposed to produce pores. Thus, the residual NaC_l particle resulted in high density and low porosity of the foam. It is clearly showed from the results that by having longer dissolution time, more NaC_l particles had been dissolved. The foam which went through the longest dissolution time (3 h) shows the lowest density and the highest porosity.

Figure 2 shows the existence of pores in A_l-40NaC_l and A_l-60NaC_l foam. It can be seen that the foam which went through 3 h of dissolution time has higher amount of pores than the other foams. This is because longer dissolution time provides enough time to dissolve more NaC_l particles. The sizes of pore in the foams were also increased by increasing the dissolution times. Details of pore characteristics are summarized in Table 1. With higher percentages of NaC_l particles, the particles become in contact with each other. During the dissolution process, the continuous connection between the NaC_l particles made them easier to be dissolved. Thus, the interconnected particles produced interconnected pores (Bin et al. 2007). However, foam with high volume fraction of NaC_l particles (A_l-60NaC_l), produced thinner cell wall because the particles are too closed to each other. In this case, during longer dissolution process, besides the NaC_l particle dissolved, thin cell walls also washed away during this process. From the Table 1, it shows that the cell wall thickness of Al-40NaC_l foam with 3 h dissolution time was 70.71 μm. Meanwhile, the cell wall thickness of Al-60NaC_l foam was 62.5 μm for the same dissolution time. Figure 3 shows optical micrographs of A_l-40NaC_l and Al-60NaC_l foams, respectively, with different dissolution times. It clearly observed that the A_l-40NaC_l foams have lesser loss cell wall than Al-60NaC_l. Besides that, higher loss cell walls were observed in Al-60NaC_l foam with 3 h dissolution time compared with foam dissolved for 1 h.

Compression test was performed on A_l-40NaC_l and A_l-60NaC_l foam fabricated with different dissolution times. The compressive stress-strain curves obtained from the foams are shown in Figures 4 and 5. The stress-strain curves of the foams showed a similar stress-strain behavior of typical aluminum foam. The curve can be characterized by three distinct regions, i.e. elastic deformation, followed by a long deformation plateau and then densification region. These foams exhibited small elastic regions,

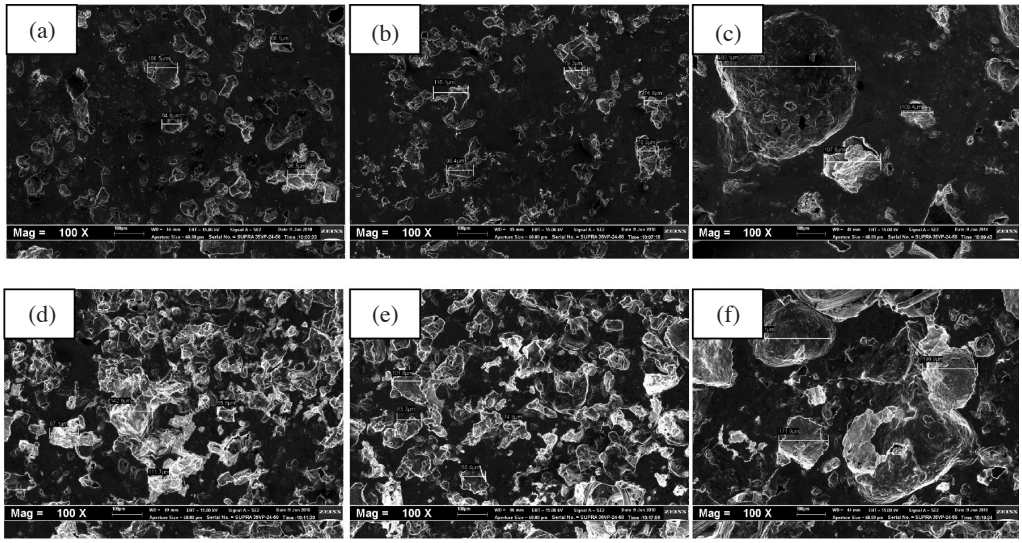

FIGURE 2. SEM micrograph of (a) A_l-40NaC_l -1 h, (b) A_l-40NaC_l -2 h, (c) A_l-40NaC_l -3 h (d) A_l-60NaC_l -1 h, (e) A_l-60NaC_l -2 h and (f) A_l-60NaC_l -3 h

TABLE 1. Pores characteristic of A_l-40NaC_l and A_l-60NaC_l foams with different dissolution times

Sample	Dissolution Times (h)	Density (g/cm^3)	Average Pore Size (μm)	Average Wall Thickness (μm)
A_l-40NaC_l	1	2.00	93.80	103.20
	2	1.87	103.25	85.68
	3	1.76	153.50	70.71
A_l-60NaC_l	1	1.44	100.34	97.20
	2	1.26	135.13	70.63
	3	1.03	172.60	62.50

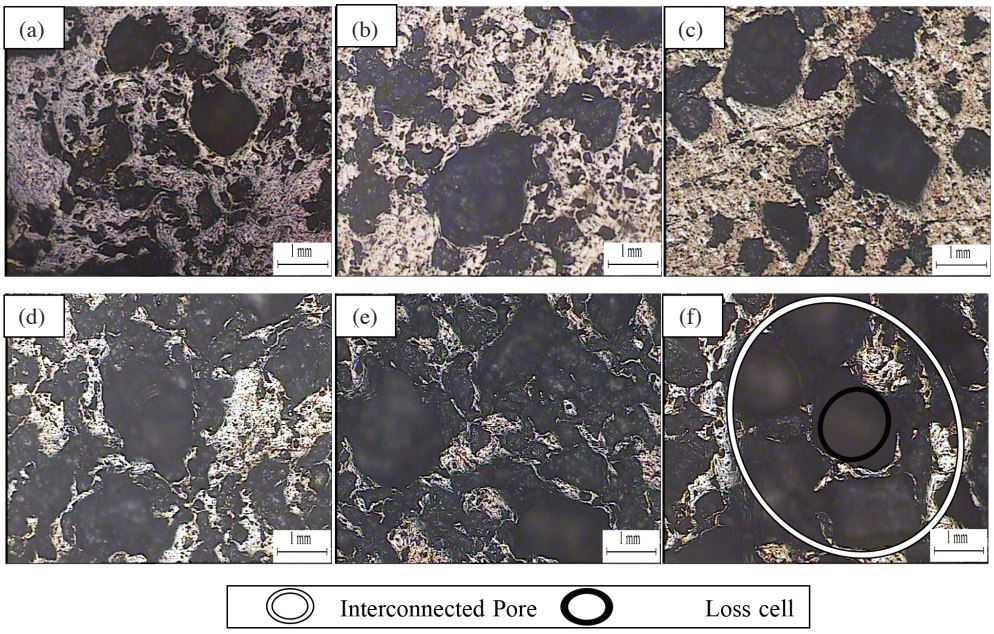

FIGURE 3. Optical micrograph of aluminum foams with different dissolution times (a) A_l-40NaC_l -1 h, (b) A_l-40NaC_l -2 h, (c) A_l-40NaC_l -3 h, (d) A_l-60NaC_l -1 h, (e) A_l-60NaC_l -2 h and (f) A_l-60NaC_l -3 h

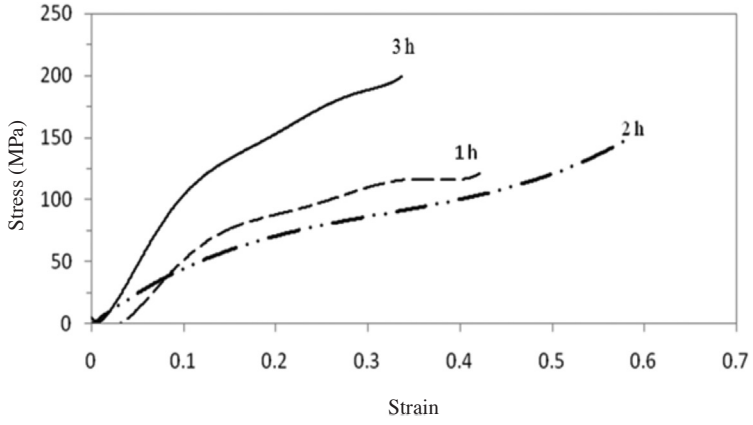

FIGURE 4. Compressive stress-strain of A_l-40NaC_l foam with different dissolution times

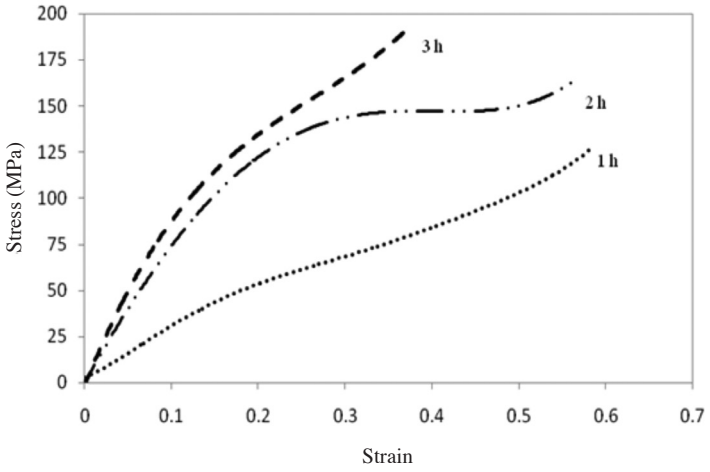

FIGURE 5. Compressive stress-strain of A_l-60NaC_l foam with different dissolution times

followed by a stress plateau, which caused by the plastic yielding and bending of cell ligaments (Neih et al. 2000; Yu et al. 2009). The compression stress-strain curve was summarized in Table 2. From these two compositions of foam, it showed that yield stress of A_l-40NaC_l foam increased with the increasing dissolution times. The higher yield stress values were associated with the high plasticity of metals (Mondal et al. 2009). Higher percentages of NaC_l residuals reduced the yield stress of A_l-40NaC_l foam due to the decreasing in ductility properties of the foam. Thus, increased dissolution time, dissolved residual NaC_l particles in A_l-40NaC_l. As a result, A_l-40NaC_l foam with the higher yield stress was formed. However, A_l-60NaC_l foam with increased dissolution time showed decreasing value of yield stress. Since, A_l-60NaC_l foam have higher amount of interconnected pores, the increasing dissolution times affected the yield stress of the A_l-60NaC_l foam. The possible explanation would be due to long dissolution process caused the loss cell wall phenomenon to occur, consequently reduced aluminum content (Han et al. 2004).

For the second region, it can be seen the extended plateau in stress-strain curve. In the deformation region, plastic deformation and the fractures of cell wall were in progressed simultaneously. It can be observed in Figures 4 and 5 that the extended plateau increased by increasing the dissolution time. The extended plateau region depends on cell types, aspect ratio of pore, cell size and its volume fraction and degree of its dispersion (Jeon et al. 2009). The morphologies of foam were important to relate the compressive properties. Foam with 2 h dissolution time of each composition showed the longer extended plateau. In morphology observation presented previously (Figure 3), the foams had homogeneous structure, higher amount of pores and larger pore size with interconnected pore. It has been proven that foam with 2 h dissolution time developed longer extended plateau. This is because the structure can absorb more energy during the cell wall collapse process. As the strain was increased further, an abrupt rise in the flow stress occurred which is also known as densification region. Here, the foam deformed as a solid material. At certain point, the rise of the stress stopped when reached the highest stress just before fracture. This point was called as compressive strength. From Table 2, it can be seen that the compressive strength of A_l-40NaC_l and A_l-60NaC_l foams shows the value of compression strength increased by increasing dissolution times. This is because when the foam went through long dissolution process, NaC_l particle dissolved completely. So, the compression load performed on the foam depends on aluminum as the main material to support the structure.

Figures 6 and 7 show the energy absorption curves of A_l-40NaC_l and A_l-60NaC_l foams with different dissolution times. The length of curves depends on the extended plateau region in the stress-strain curve. From energy absorption

TABLE 2. Stress-strain curve characteristics of A_l-40NaC_l and A_l-60NaC_l foam with different dissolution times

Sample	Dissolution times (h)	Compressive strength (MPa)	Offset yield stress (MPa)	Yield strain	Modulus (GPa)
A_l-40NaC_l	1	120.107	60.173	0.108	1.291
	2	163.003	82.061	0.107	0.831
	3	196.272	98.531	0.094	1.204
A_l-60NaC_l	1	126.744	110.121	0.295	0.192
	2	160.960	84.400	0.114	0.755
	3	184.400	96.702	0.113	0.875

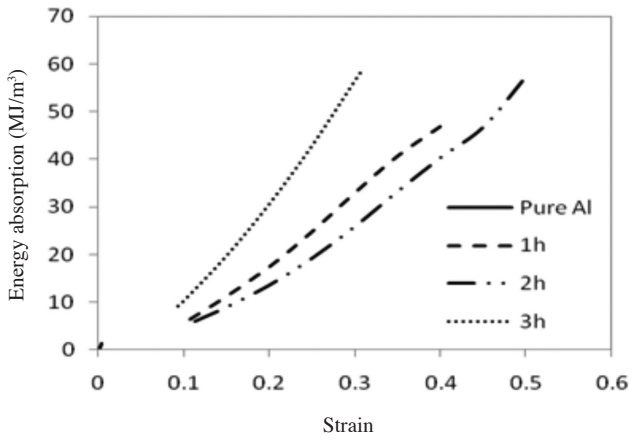

FIGURE 6. Energy absorption curve of A_l-40NaC_l with different dissolution times

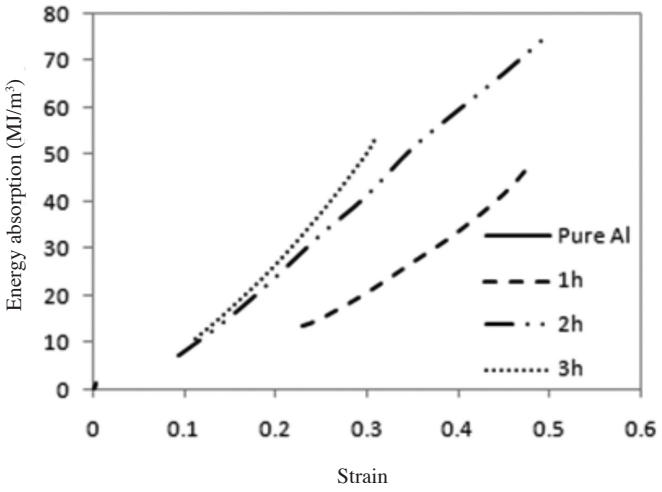

FIGURE 7. Energy absorption curve of A_l-60NaC_l with different dissolution times

curves of A_l-40NaC_l and A_l-60NaC_l foams, it showed that the energy absorption increased with increasing strain. The 2 h dissolution times showed the longer energy absorption curve which suggested that this foam have higher energy absorption. The total energy absorption for 2 h dissolution foams was the highest compared with other foam which can be observed in Figures 6 and 7.

There are several reasons of this finding. The 2 h dissolution time was enough for the entire NaC_l particle to be completely dissolved. This 2 h process also produced foam with larger size of pores. Meanwhile, it was found that the aluminum foam which went through 3 h dissolution time had the lowest energy absorption although it has highest compression strength. This showed that 3 h dissolution time was too long for dissolving the NaC_l until the aluminum body was dissolved as well. This suggestion was based on SEM observation for foam with 3 h dissolution time which have higher amount of loss cell wall (Figure 2). This finding showed that the structure of the foam was weak to support the loading stress. During the dissolution process the cell wall also washed away and longer time caused more cell wall to be washed away. By comparing the two compositions of foam, A_l-40NaC_l and A_l-60NaC_l foams showed higher energy absorption when dissolved at 1 and 2 h. As a cellular material, porosity and pore structure were main factors affected properties of the foam. Therefore, appropriate selection of dissolution times was required to obtain good absorber foam. The dissolution times selected should completely dissolved NaC_l particles without lots of loss cell wall which resulting in low energy absorbing performance. Therefore, the suitable dissolution time for A_l-40NaC_l and A_l-60NaC_l foams was 2 h which proved by its highest energy absorption capability.

CONCLUSION

The aluminum foams with different dissolution times were successfully fabricated by sintering dissolution process. The foams with average pore sizes of 1 mm were produced by sintering dissolution process using NaC_l as foaming agent. Increasing percentages of foaming agent increased the pore structures, which leads to lightweight foam. The density of A_l foam was reduced by dissolution process for 3 h. Compression strength of aluminum foam was improved as dissolution time increased from 1 to 3 h. It was found that 2 h dissolution time showed higher energy absorption as presented longest plateau region compared with other dissolution times. This is due to NaC_l particles completely dissolved at 2 h dissolution time. It showed that by increasing dissolution times, compressive properties and energy absorption of foam increased. However, foam with 3 h dissolution time has the lowest energy absorption due to higher amount of loss cell wall during dissolution process.

ACKNOWLEDGEMENTS

The authors gratefully acknowledge the financial support from Universiti Sains Malaysia (1001/PBahan/8032019).

REFERENCES

Andrews, E., Sanders, W. & Gibson, L. 1999. Compressive and tensile behaviour of aluminum foams. *Materials Science and Engineering A* 270: 113-124.

Bin, J., Zejun, W. & Naiqin, Z. 2007. Effect of pore size and relative density on the mechanical of open-cell aluminum alloy foams. *Scripta Materialia* 56: 169-172.

Cao, X.Q., Wang, Z.H., Ma, H.W., Zhao, L.M. & Yang, G.T. 2006. Effects of heat treatment on dynamic compressive properties and energy absorption characteristics of open-cell aluminum alloy foams. *Transactions of Nonferrous Metals Society of China* 16: 159-163.

Fusheng, H., Cheng, H., Wang, J. & Wang, Q. 2004. Effect of pore combination on the mechanical properties of an open cell aluminum foam. *Scripta Materialia* 50: 13-17.

Gaillard, C., Despois, J.F. & Mortensen, A. 2004. Processing of NaC_l powders of controlled size and shape for the microstructural tailoring of aluminium foams. *Materials Science and Engineering A* 374: 250-262.

Haijun, Y., Zhiqiang, G., Bing, L., Guangchun, Y., Hongjie, L. & Yihan, L. 2007. Research into the effect of cell diameter

of aluminum foam on its compressive and energy absorption properties. *Materials Science and Engineering A* 454-455: 542-546.

Han, F., Cheng, H., Wang, J. & Wang, Q. 2004. Effect of pore combination on the mechanical properties of an open cell aluminium foam. *Scripta Materialia* 50: 13-17.

Jeon, Y.P., Kang, C.G. & Lee, S.M. 2009. Effect of cell size on compression and bending strength of aluminum-foamed material by complex stirring in induction heating. *Journal of Materials Processing Technology* 209: 435-444.

Miranda, V., Teixeira-Dias, F., Pinho-da-Cruz, J. & Novo, F. 2010. The role of plastic deformation on the impact behaviour of high aspect ratio aluminium foam-filled sections. *International Journal of Non-Linear Mechanics* 45: 550-561.

Mondal, D.P., Goel, M.D. & Das, S. 2009. Compressive deformation and energy absorption characteristics of closed cell aluminum-fly ash particle composite foam. *Materials Science and Engineering A* 507: 102-109.

Nieh, T.G., Higashi, K. & Wadsworth, J. 2000. Effect of cell morphology on the compressive properties of open cell aluminum foams. *Materials Science and Engineering A* 283: 105-110.

Wang, Z., Ma, H., Zhao, L. & Yang, G. 2006. Studies on the dynamic compressive properties of open-cell aluminum alloy foams. *Scripta Materialia* 54: 83-87.

Xiao-Qing, C., Zhi-Hua, W., Hong-Wei, M., Long-Mao, Z. & Gui-Tong, Y. 2006. Effects of cell size on compressive properties of aluminium foam. *Transactions of Nonferrous Metals Society of China* 16: 351-356.

Yu, S., Liu, J., Wei, M., Luo, Y., Zhu, X. & Liu, Y. 2009. Compressive property and energy absorption characteristic open cell ZA22 foam. *Material and Design* 30: 87-90.

Zhang, C.J., Feng, Y. & Zhang, Z. 2010. Mechanical properties and energy absorption properties of Aluminum foam-filled square tubes. *Transactions of Nonferrous Metals Society of China* 2: 1380-1386.

Zhao, Y.Y. & Sun, D.X. 2001. A novel sintering-dissolution process for manufacturing A_l foams. *Scripta Materialia* 44: 105-110.

School of Materials and Mineral Resources Engineering
Engineering Campus, Universiti Sains Malaysia
14300 Nibong Tebal, Pulau Pinang
Malaysia

*Corresponding author; email: anasyida@eng.usm.my

Received: 23 March 2012
Accepted: 23 May 2012